TELKOMNIKA Telecommunication Computing Electronics and Control
Vol. 24, No. 1, February 2026, pp. 1~13
ISSN: 1693-6930, DOI: 10.12928/TELKOMNIKA.v24i1.27236

Deep learning-based power amplifier linearization in OFDM systems with unknown channel state information

Meryem Mamia Benosman, Mohammed Yassine Bendimerad, Fethi Tarik Bendimerad
LTT laboratory, Department of Telecommunication, Faculty of Technology, University of Tlemcen, Chetouane, Algeria

Article Info

Article history:

Received May 22, 2025
Revised 25 Oct, 2025
Accepted Dec 8, 2025

Keywords:

Autoencoder
Deep learning
Digital predistortion
Orthogonal frequency-division multiplexing
Power amplifiers

ABSTRACT

This paper presents an end-to-end deep learning-based approach for orthogonal frequency-division multiplexing (OFDM) communication systems impaired by nonlinear power amplifiers (PAs) and channel fading. The PA nonlinearity is modeled using the modified Rapp model, and simulations are performed on a 64-subcarrier OFDM system with a cyclic prefix (CP) of 8 and 16-quadrature amplitude modulation (16-QAM). The proposed autoencoder-based OFDM–PA (AE-OFDM-PA) system jointly optimizes the transmitter and receiver through end-to-end learning, enabling simultaneous compensation of both PA nonlinearities and channel distortions without requiring explicit channel state information (CSI) estimation. Instead, the model leverages embedded pilot sequences to learn the implicit CSI representation directly from data, allowing the receiver to correct amplitude and phase distortions adaptively. Simulation results demonstrate that AE-OFDM-PA significantly outperforms conventional OFDM and OFDM-PA systems, achieving over 70× block error rate (BLER) improvement compared with the uncompensated OFDM-PA system at an input back-off (IBO) of 3 dB. Furthermore, the proposed method achieves approximately 11.5 dB adjacent channel leakage ratio (ACLR) improvement over the classical memory polynomial digital predistortion (DPD) technique, while slightly reducing the peak-to-average power ratio (PAPR). Overall, AE-OFDM-PA provides a robust, spectrally efficient, and low-complexity solution for nonlinear and fading environments with unknown or varying CSI.

Corresponding Author:

Meryem Mamia Benosman
LTT laboratory, Department of Telecommunication, Faculty of Technology
University of Tlemcen
Chetouane, Algeria
Email: meryemmamia.benosman@univ-tlemcen.dz

1. INTRODUCTION

The continuous evolution of wireless communication technologies has dramatically increased mobile connectivity and global data traffic. By 2023, the number of IP-connected devices exceeded three times the world's population, with an average of 3.6 networked devices per person, up from 2.4 in 2018 [1]. This growth is expected to continue with the deployment of fifth-generation (5G) and emerging sixth-generation (6G) networks, which aim to deliver data rates up to 20 Gb/s and end-to-end latency below 10 ms [2].

These systems rely heavily on multicarrier modulation techniques such as orthogonal frequency-division multiplexing (OFDM) [3], known for its robustness against multipath fading and inter-symbol interference (ISI) [4]. However, OFDM signals exhibit a high peak-to-average power ratio (PAPR), which leads to severe signal distortion when amplified by nonlinear power amplifiers (PAs) [5]. Operating PAs near

saturation improves power efficiency but causes in-band distortion and out-of-band spectral regrowth, resulting in bit error rate (BER) degradation and adjacent-channel interference. This trade-off between efficiency and linearity has been extensively studied in recent literature [6].

Various PAPR reduction techniques have been proposed, including clipping, selective mapping (SLM), partial transmit sequence (PTS), tone reservation (TR), tone injection (TI), and active constellation extension (ACE) [7]-[11]. Although these methods effectively reduce PAPR, they often increase system complexity or introduce additional distortion. Therefore, digital predistortion (DPD) remains one of the most practical and efficient approaches for PA linearization, as it compensates for nonlinearities by applying an inverse transfer function prior to amplification.

Recently, deep learning-based models have demonstrated outstanding capabilities in modeling nonlinearities and compensating signal distortions thanks to their strong function approximation properties [12]. Architectures such as convolutional neural networks (CNNs), long short-term memory (LSTM) networks, generative adversarial networks (GANs), and autoencoders (AEs) [13]-[16] have been explored for transmitter optimization, PA linearization, and signal restoration.

In this work, we propose an autoencoder-based OFDM-PA (AE-OFDM-PA) system that performs end-to-end learning to jointly linearize the nonlinear response of a modified Rapp-based PA and to compensate for Rayleigh fading. Unlike conventional DPD approaches, the proposed model learns the optimal mapping between transmitted and received signals directly through data-driven training, achieving both distortion mitigation and low computational complexity.

The remainder of this paper is organized as follows. Section 2 presents the proposed methodology, including the system model and AE-based DPD framework. Section 3 discusses the simulation results and comparative analysis. Finally, section 4 concludes the paper and outlines possible directions for future work.

2. METHODOLOGY

2.1. Overview of existing techniques

DPD is widely adopted as an effective technique for power amplifier linearization. Conventional DPD schemes, such as look-up table (LUT), Volterra series, and memory polynomial models [17], [18], attempt to approximate the inverse behavior of the PA and apply it before amplification. However, their performance is limited by modeling accuracy, sensitivity to memory effects, and dependence on parameter tuning. Recent advances in deep learning have introduced data-driven approaches capable of directly learning complex nonlinear mappings from data [19]. Architectures such as CNNs, LSTMs, and autoencoders AEs have shown promising results for PA linearization and end-to-end transmitter optimization. The proposed AE-OFDM-PA model builds upon this paradigm by leveraging an AE-based framework to jointly mitigate PA nonlinearities and channel distortions while maintaining low computational complexity.

2.2. System model and classical digital predistortion

2.2.1. OFDM signal model

OFDM is a multicarrier modulation technique that enables high data rates and robustness against ISI. The baseband OFDM signal is generated using the inverse discrete Fourier transform (IDFT) [20], which maps frequency-domain modulation symbols to the time domain as:

$$x(t) = \frac{1}{\sqrt{N}} \sum_{k=0}^{N-1} X_k \, e^{j2\pi f_k t}, 0 \le t \le NT \quad (1)$$

where N denotes the number of subcarriers, X_k is the transmitted symbol on the k-th subcarrier, f_k is the frequency of the k-th subcarrier and T is the OFDM symbol duration.

A cyclic prefix (CP) is inserted by copying the end of each symbol to its beginning to maintain orthogonality in multipath channels. At the receiver, the CP is removed, and channel equalization enables the recovery of transmitted data symbols. A significant challenge in OFDM is the presence of a non-constant envelope, characterized by high power peaks compared to the average signal power. Specifically, as the number of subcarriers N increases, the signal $x(t)$ follows a complex Gaussian process based on the central limit theorem (CLT) [21]. To measure, the amplitude fluctuations in the OFDM signal, the peak to average power ratio is commonly employed. The PAPR ratio is expressed as:

$$PAPR = 10 \, log_{10} \left(\frac{\underset{0 \le n \le N-1}{max} |x(t)|^2}{\mathbb{E}[|x(t)|^2]} \right) \quad (2)$$

where, $\mathbb{E}\{.\}$ is the statistical expectation operator, and $x(t)$ is the baseband OFDM signal in the time domain.

The probability that the PAPR exceeds a given threshold δ is characterized using the complementary cumulative distribution function (CCDF):

$$CCDF[PAPR(x(t))] = prob[PAPR(x(t)) > \delta] \quad (3)$$

where $prob[.]$ denotes the probability operator, and δ is the PAPR threshold. A large PAPR can drive nonlinear components such as power amplifiers into saturation, causing signal distortion and spectral regrowth.

2.2.2. Power amplifier model (Rapp modified)

The power amplifier is an essential component in the transmission chain as it is responsible for amplifying the signal. Its behavior is described by its transfer function, which defines the relationship between the input and output signals. The amplitude modulation to amplitude modulation (AM/AM) characteristic indicates how the amplitude of the output signal varies with respect to the input signal's amplitude. On the other hand, AM/PM characteristic describes the phase shift between the input and output signals [22]. The amplified signal can be expressed as:

$$x_{amp}(t) = F\big(x(t)\big) = F_A(\rho(t))e^{j\left(\theta(t)+F_\theta(\rho(t))\right)} \quad (4)$$

where, $\rho(t)$ and $\theta(t)$ are respectively the modulus and the phase of the signal $x(t)$. $F_A(.)$ describes the AM/AM conversion and $F_\theta(.)$ describes AM/PM conversion of the amplifier.

In this study, the Rapp modified model is employed to represent the static nonlinear behavior of the PA. It captures both AM/AM and AM/PM distortions as follows. Figure 1(a) illustrates the AM/AM characteristic of the Rapp modified model and Figure 1(b) shows AM/PM characteristics.

$$F\big(\rho(t)\big) = \frac{G_a\rho(t)}{\left(1+\left(\frac{G_a\rho(t)}{V_{sat}}\right)^{2p}\right)^{\frac{1}{2p}}} \quad (5)$$

$$F(\rho(t))_\theta = \frac{A(\rho(t))^q}{1+\left(\frac{\rho(t)}{A'}\right)^q} \quad (6)$$

where, $\rho(t)$ is the modulus of the input OFDM signal, G_a is the PA gain. The parameter p adjusts the characteristic by controlling the transition between the linear area and the saturation area of the AM/AM characteristic. V_{sat} is the saturation voltage of the PA. The A and A' parameters control the level of phase distortion introduced by the PA.

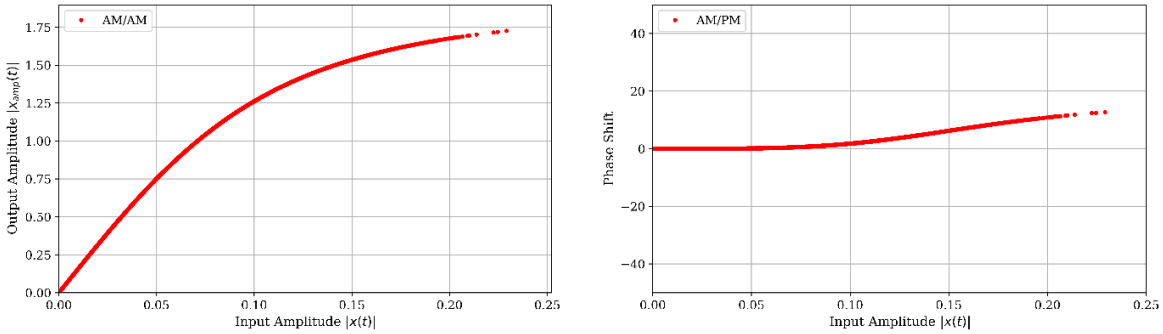

(a) (b)

Figure 1. Characteristics of the modified Rapp model: (a) AM/AM conversion and (b) AM/PM conversion

The input back-off (IBO) is an important parameter that defines the operating point of the amplifier relative to its saturation level. It is expressed as the ratio between the saturation power P_{sat} and the average input power. A higher IBO value indicates that the amplifier operates in a more linear region, ensuring lower distortion but reduced power efficiency, while a lower IBO value increases efficiency at the cost of stronger nonlinear effects. The IBO is mathematically defined as:

$$IBO(dB) = 10\log_{10}\left(\frac{P_{sat}}{\mathbb{E}[|x(t)|^2]}\right) \quad (7)$$

where, P_{sat} denotes the saturation power of the PA, $\mathbb{E}[|x(t)|^2]$ denotes the average input power.

2.2.3. Classical memory polynomial DPD

To compensate for PA nonlinearities, DPD techniques are applied before amplification. The principle is to introduce a nonlinear inverse function, denoted as $P(.)$, such that the cascade $P(.)F(.)$ (predistorter followed by amplifier) behaves approximately linearly. The concept is depicted in Figure 2.

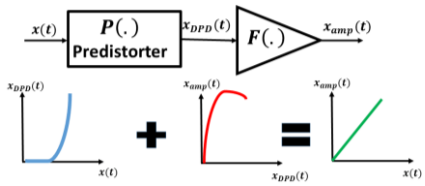

Figure 2. Digital predistortion mechanism for power amplifier linearization

In this work, the memory polynomial model is adopted as a classical benchmark for PA linearization. The predistorted signal $x_{DPD}(t)$ is expressed as:

$$x_{DPD}(t) = \sum_{i=0}^{I-1}\sum_{l=1,3,5,..}^{L} a_{l,i}x(t-i)|x(t-i)|^{l-1} \quad (8)$$

where, L denotes the polynomial order, I the memory depth, and $a_{l,i}$ the complex coefficients obtained via least squares estimation.

In the implemented algorithm, the basis functions are built from the PA output signal, and the coefficients are optimized to approximate the inverse of the amplifier's nonlinear response. This approach, known as memory polynomial DPD, offers a good trade-off between performance and computational complexity, making it widely used in practical radio frequency (RF) systems [23]. However, its effectiveness decreases for highly nonlinear or memory-intensive PAs, motivating the use of deep learning–based DPD architectures explored in this paper.

2.3. End-to-end learning for communication systems

Deep learning has emerged as a transformative tool in communication systems, offering the ability to model complex nonlinear relationships through data-driven learning. Rather than designing each block of the transmission chain separately, the end-to-end learning paradigm trains the entire system jointly, from the transmitter to the receiver, through differentiable models.

The concept was first inspired by the structure of autoencoders AEs, where the encoder represents the transmitter, the channel acts as a stochastic layer introducing impairments, and the decoder represents the receiver. The network is trained to minimize the difference between the transmitted and recovered messages, thus automatically learning optimal signal representations for the given channel and hardware impairments.

Recently, several neural DPD frameworks have been proposed, including CNN- and LSTM-based architectures as well as temporal convolutional networks (TCN)-DPD for modeling PA nonlinearities and memory effects [24], [25]. However, most of these approaches treat predistortion and equalization as separate tasks. In contrast, the proposed AE-OFDM-PA framework jointly performs PA linearization and channel compensation in an end-to-end learning process, providing enhanced robustness and adaptability without explicit CSI modeling.

2.3.1. Autoencoder principle

An autoencoder is a type of neural network designed for unsupervised end-to-end learning [26]. It learns to reconstruct its input s at the output $\hat{s}$ after passing through a bottleneck representation:

$$\hat{s} = \sigma(W_h s_{h-1} + b_h)\ ;\ h = 1, \dots, H \quad (9)$$

where, W_h and b_h denote the weight matrix and bias vector, $\sigma(.)$ is the activation function and H the number of hidden layers.

The encoder $f(s)$ maps the input data into a latent representation, while the decoder $g(s)$ reconstructs it as presented in Figure 3. Common activation functions include the ReLU**,** sigmoid, linear, and SoftMax functions.

Training aims to minimize the categorical cross-entropy loss**:**

$$\mathcal{L}(s,\hat{s}) = -\sum_j s_j \log(\hat{s}_j) \quad (10)$$

where, s and $\hat{s}$ are the true and predicted one-hot encoded symbols, respectively, Network parameters $\theta(W,b)$ are optimized using stochastic gradient descent (SGD) [27]:

$$\theta^+ = \theta - \mu\nabla_\theta \mathcal{L}(s,\hat{s}) \quad (11)$$

The transmitter's output is constrained to satisfy average power or amplitude limits, such as $\mathbb{E}[|x(t)|^2] \leq 1$. As illustrated in Figure 4, this structure allows the autoencoder to act as a complete communication system, with the encoder functioning as the transmitter, and the decoder as the receiver.

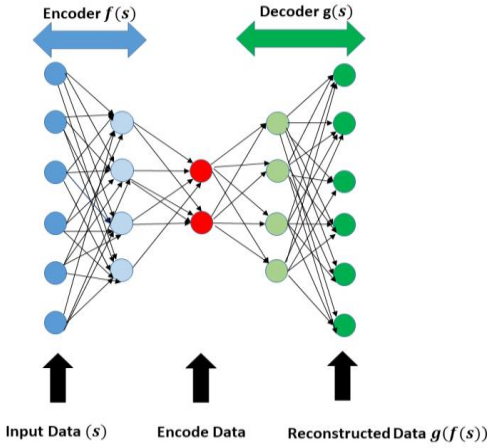

Figure 3. Architecture of an autoencoder for latent representation learning

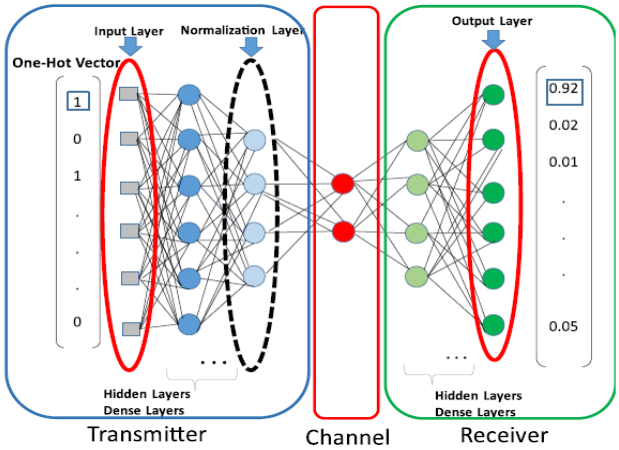

Figure 4. Autoencoder architecture for end-to-end communication system design

2.4. Proposed AE-OFDM-PA framework

We propose an end-to-end autoencoder-based OFDM system (AE-OFDM-PA) that jointly mitigates nonlinear power amplifier distortions and Rayleigh channel effects. The model, shown in Figure 5, integrates an AE-TX (encoder) and an AE-RX (decoder) trained together through end-to-end learning. A modified Rapp model is used to emulate PA nonlinearity, while embedded pilot sequences allow the AE-RX to estimate the channel implicitly, eliminating the need for explicit CSI estimation. By learning from data, the AE-OFDM-PA system compensates both amplitude and phase distortions, achieving joint linearization and channel equalization. This data-driven approach enhances robustness and spectral efficiency compared with conventional DPD methods that rely on explicit PA or channel modeling. The AE-OFDM-PA model in Figure 5 includes:

1. One AE-TX block per subcarrier: for 16-QAM modulation
2. A real/complex conversion block: for converting modulated output into complex symbols
3. A modulation block by inverse fast Fourier transform (IFFT): for symbol modulation
4. A cyclic prefix addition block: for eliminating inter symbol interference caused by the multipath channel
5. A power amplifier addition block
6. A parallel/serial conversion block
7. A complex/real conversion block
8. A channel block: Rayleigh channel one-tap
9. A real/complex conversion block
10. A serial/parallel conversion block
11. A cyclic prefix removal block
12. A FFT demodulation block

13. An equalization block for each output of the previous block
14. A complex/real conversion block
15. An AE-RX block for each subcarrier: for symbol demodulation, this block has the same architecture as a single-carrier receiver
16. A parallel/serial conversion block: to recover the sequence of binary words.

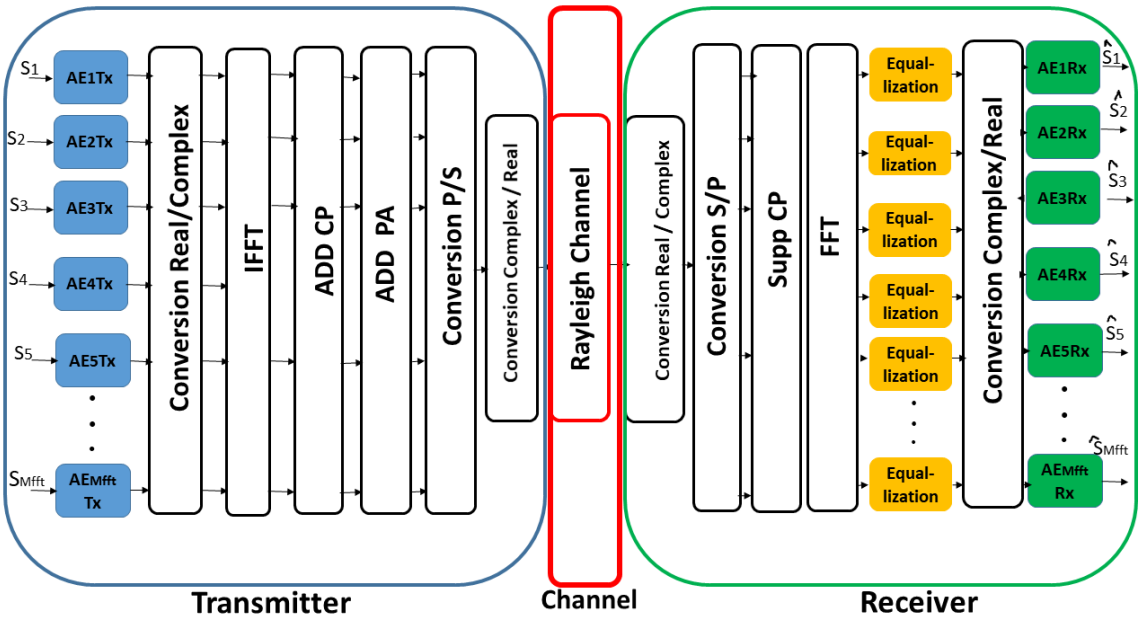

Figure 5. Detailed structure of AE-OFDM-PA

2.4.1. Channel equalization

To enable channel estimation within the AE-RX, pilot sequences are inserted into the OFDM frame. These pilots are known to both transmitter and receiver, and are orthogonal to data symbols to prevent interference. The estimated channel E_s is obtained as:

$$E_s = PI_r \frac{PI_e^*}{|P_{Ie}|^2} \tag{12}$$

where, E_s is the estimated channel, PI_e and PI_r represent the transmitted and received pilot symbols, respectively.

The AE-RX receives four inputs, the real and imaginary parts of the received signal (y_{c_r}, y_{c_i}), and the real and imaginary parts of the estimated channel (E_{s_r}, E_{s_i}), as depicted in Figure 6**.** This configuration enables the AE-RX to jointly correct amplitude and phase distortions by learning to exploit the implicit CSI rather than relying on explicit analytical channel models.

During training, the autoencoder is fed with batches of size B, each containing OFDM frames augmented with identical pilot sequences across all subcarriers. Gradients are computed for each batch to update the network parameters $\theta(W, b)$ via stochastic gradient descent, ensuring stable convergence and consistent channel compensation, as illustrated in Figure 7. Once trained, the AE-OFDM-PA system exhibits a linearized end-to-end transfer function that effectively compensates for both PA nonlinearity and channel distortions without explicit CSI modeling. This data-driven learning approach enhances robustness and adaptability compared to traditional DPD methods that depend on accurate analytical models or explicit channel information.

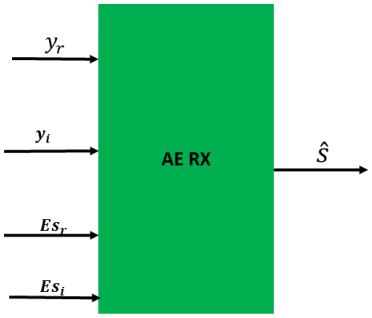

Figure 6. Principle of channel equalization

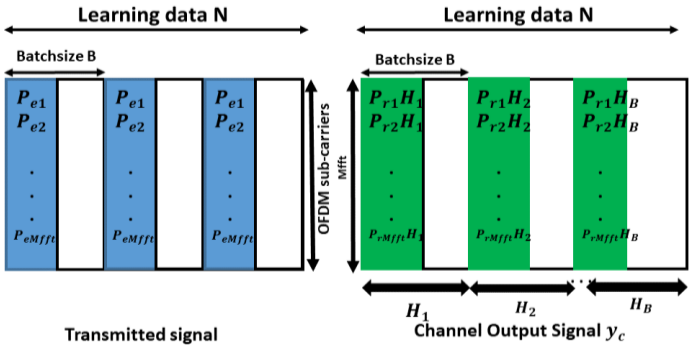

Figure 7. Structure of the pilots in the batchsize

3. RESULTS AND DISCUSSION

The training dataset used in this study was entirely generated through numerical simulations in Python, using TensorFlow and Keras libraries. The simulated dataset is based on an OFDM system comprising 64 subcarriers and a CP length of 8, modulated with 16-QAM symbols. The signal passes through a one-tap Rayleigh fading channel and a nonlinear power amplifier PA modeled by the modified Rapp model. The amplifier parameters are: Ga=16, $Vsat$=1.9, p=1.1, q=4, A=345, and A'=0.17. A total of 1,024,000 OFDM **s**ymbols were generated for training, organized in batches of 8,000 samples each. The AE-OFDM-PA network was trained over 500 epochs using the Adam optimizer.

For generalization and testing, 5000 OFDM symbols were transmitted over 5,000 independent Rayleigh channel realizations, and all performance metrics are averaged across these realizations to ensure statistical reliability. In addition, the performance of the proposed AE-OFDM-PA system was compared with a conventional memory polynomial (MP) digital predistortion (OFDM-DPD) approach, configured with a polynomial order of 7 and a memory depth of 1.

This synthetic dataset ensures full control over both channel and PA characteristics, guaranteeing reproducibility and enabling a fair comparison between the proposed deep learning–based predistortion scheme and the classical MP-DPD method.

Table 1 presents the parameters of the AE-OFDM-PA layers and the corresponding training configuration. This synthetic dataset allows full control over both channel and PA characteristics, ensuring reproducibility and enabling performance assessment of the proposed AE-OFDM-PA model under various nonlinear and fading conditions.

Table 1. Architecture of the proposed AE-OFDM-PA model

Layer	Number of neurons	Layer type	Activation function
Input layer	/	Lambda	/
Hidden layers (2)	160 per layer	Dense	ReLU
Normalization	/	Batch normalization	Linear
Conversion real/complex	2 per layer	Dense	/
IFFT	/	Lambda	/
Add CP	/	Lambda	/
PA	/	Lambda	/
Rayleigh channel	/	Lambda	/
Supp CP	/	Lambda	/
FFT	/	Lambda	/
Hidden layers (2)	160 per layer	Dense	ReLU
Output layer	16 per layer	Dense	Softmax

3.1. Constellation results

The constellation analysis in Figure 8 compares the proposed AE-OFDM-PA system (Figure 8(a)) with the conventional OFDM-DPD scheme (Figure 8(b)) under a highly nonlinear condition, where the PA operates near saturation (IBO=3 dB). In the conventional OFDM-DPD system, the objective is to preserve the standard 16-QAM constellation at the PA input (blue points). The DPD block compensates for the nonlinear behavior of the amplifier, improving the received constellation (green) compared with the severely distorted output after the PA and channel (red). However, this approach depends on accurate PA modeling and acts as an external correction module.

In contrast, the AE-OFDM-PA framework employs an end-to-end learning strategy that jointly optimizes transmission and reception. The AE-TX learns a non-standard constellation at the transmitter (blue) that is inherently robust to nonlinearities, while the AE-RX reconstructs a clean 16-QAM-like constellation (green) at the receiver despite strong distortion (red). This behavior demonstrates that the AE-OFDM-PA not only compensates for PA and channel impairments but also learns to adapt its modulation scheme to maximize robustness under harsh nonlinear conditions such as IBO=3 dB. These findings confirm the effectiveness of the joint AE-TX/AE-RX optimization in mitigating nonlinear distortions without requiring explicit PA modeling.

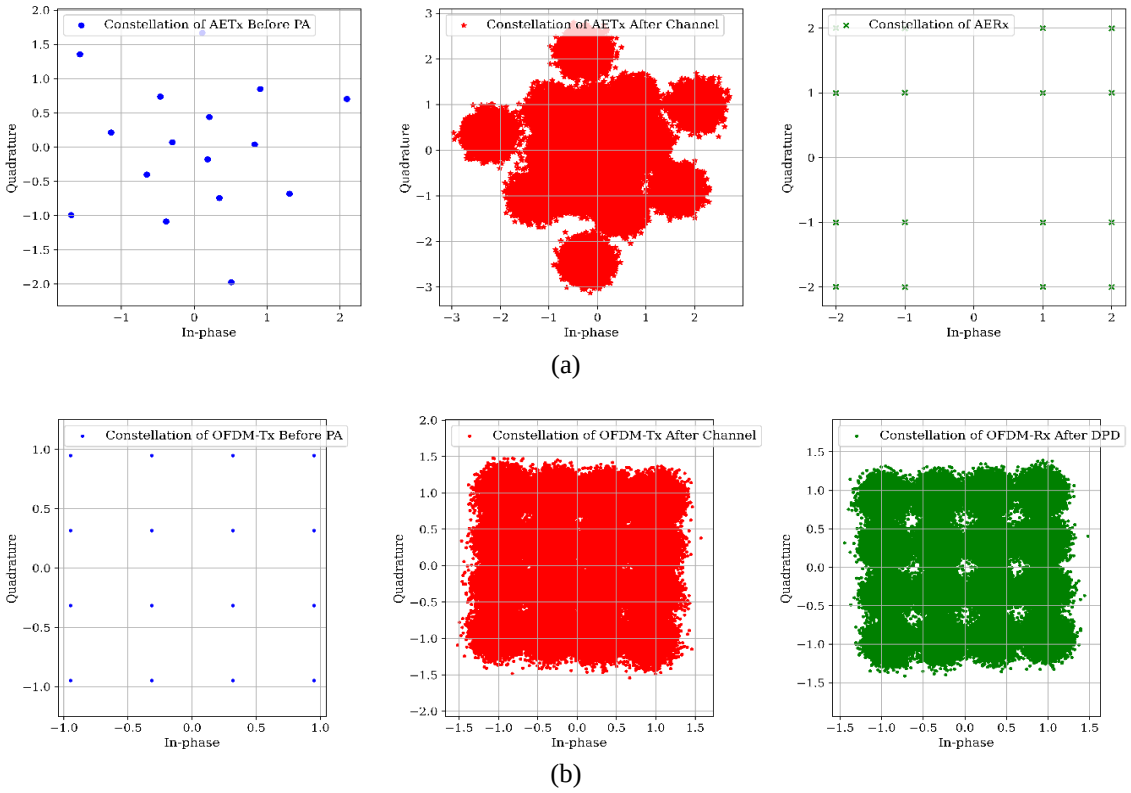

Figure 8. Constellation comparison of (a) AE-OFDM-PA and (b) OFDM-DPD

3.2. Block error rate (BLER) results

A detailed comparison of the BLER performance was carried out among the proposed AE-OFDM-PA system, the conventional OFDM and OFDM-PA schemes, and the reference OFDM-DPD approach. The results, presented in Figure 9, assess the robustness of these systems under severe nonlinear distortion conditions, with the PA operating at an IBO of 3 dB. To ensure high statistical accuracy, the simulation setup was refined to enable reliable BLER estimation down to 10^{-5}. The OFDM-PA curve (red) shows a clear performance degradation due to the amplifier's nonlinearity, reaching an error floor above 3×10^{-2} at high Eb/N0 values.

In contrast, the OFDM-DPD system (green) effectively compensates for these nonlinearities, achieving performance comparable to the ideal OFDM reference (magenta), which represents the upper bound for linearization. The proposed AE-OFDM-PA model (cyan) exhibits a strong ability to mitigate both nonlinear and channel-induced impairments. At $Eb/N0$=20 dB, it achieves a BLER of approximately 5×10^{-4}, corresponding to more than a 70-fold improvement over the uncompensated OFDM-PA. Although its performance does not exactly match that of the analytically modeled DPD, the AE-OFDM-PA remains highly competitive. At a target BLER of 10^{-3}, it requires only about 2 dB higher Eb/N0 than the optimized OFDM-DPD reference. These findings validate the capability of the proposed end-to-end learning framework to preserve signal integrity and confirm that deep learning-based compensation can serve as a robust and model-free alternative to traditional DPD methods.

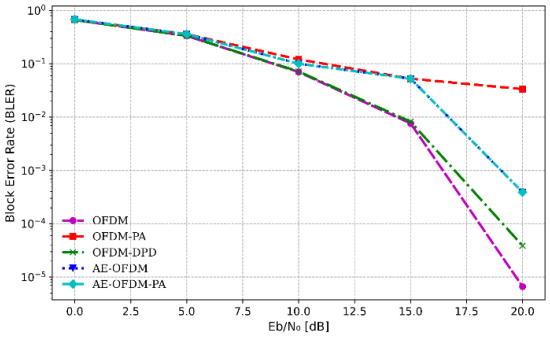

Figure 9. BLER performance for different OFDM-based systems

3.3. Analysis of power spectral density and adjacent channel leakage ratio

The performance of the AE-OFDM-PA system was also evaluated in the frequency domain using two key spectral metrics: the power spectral density (PSD) and the adjacent channel leakage ratio (ACLR). As shown in Figure 10, the PSD reveals the impact of the PA nonlinearity on spectral spreading under the challenging IBO = 3 dB condition. In the conventional OFDM-PA system, strong nonlinearity causes significant spectral regrowth, raising the out-of-band noise floor to about −10.5 dB/Hz (at normalized frequency ±0.4). When a conventional DPD based on a memory polynomial model is applied, a slight reduction is observed, improving the out-of-band level to approximately −14 dB/Hz. However, this improvement remains limited, particularly for signals exhibiting memory effects.

In contrast, the proposed AE-OFDM-PA system effectively suppresses spectral regrowth, maintaining the out-of-band level close to −20 dB/Hz, which is nearly identical to that of an ideal linear system. This represents an improvement of about 9.5 dB over the uncompensated OFDM-PA and nearly 6 dB over the conventional DPD. These results demonstrate that the autoencoder is capable of learning a signal representation that inherently minimizes spectral distortion despite hardware nonlinearities.

The ACPR results, shown in Figure 11, further confirm these findings. The vertical axis represents the ACPR measured in dB at the PA output, while the horizontal axis corresponds to the different OFDM-based transmission schemes. The uncompensated OFDM-PA system exhibits the strongest degradation (≈−12.5 dB), while the conventional DPD achieves only moderate improvement (≈−7.0 dB). By comparison, the AE-OFDM-PA system achieves an ACLR of approximately −18.5 dB, corresponding to gains of about 6 dB and 11.5 dB over the OFDM-PA and DPD systems, respectively.

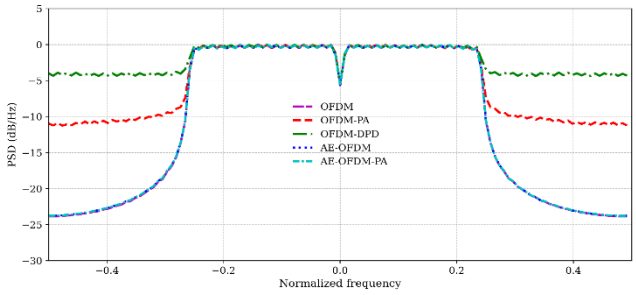

Figure 10. PSD performance for different OFDM-based systems

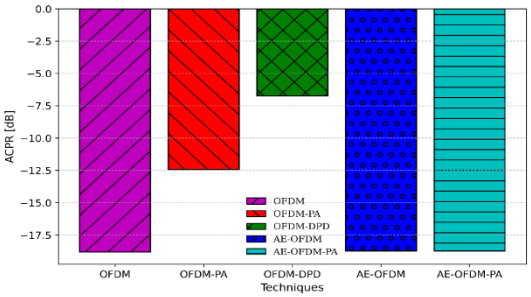

Figure 11. Comparison of ACPR performance highlighting AE-OFDM-PA and OFDM-DPD schemes

Overall, these spectral results confirm that the AE-OFDM-PA approach not only reduces spectral regrowth to near-ideal levels but also provides the highest measurable gain in ACLR. This makes it a more robust and spectrally efficient alternative to conventional linearization techniques. It should be noted that all results were obtained from simulations without hardware-in-the-loop or real PA measurements. Future work will focus on experimental validation using RF hardware and extensions to more complex scenarios, including amplifiers with memory effects, multiple-input multiple-output (MIMO) configurations, and wideband fading channels.

3.4. Analysis of the CCDF and PAPR

Figure 12 presents the CCDF, a key metric used to assess the system's PAPR and its resilience to power compression. The results show that introducing an end-to-end learning approach with autoencoder networks does not adversely affect the PAPR performance. The AE-OFDM (blue) and conventional OFDM (magenta) curves are nearly identical, both exhibiting a PAPR of approximately 10.2 dB at a probability of 10^{-3}. This observation confirms that the AE-OFDM-PA design preserves the intrinsic power characteristics of the transmitted signal.

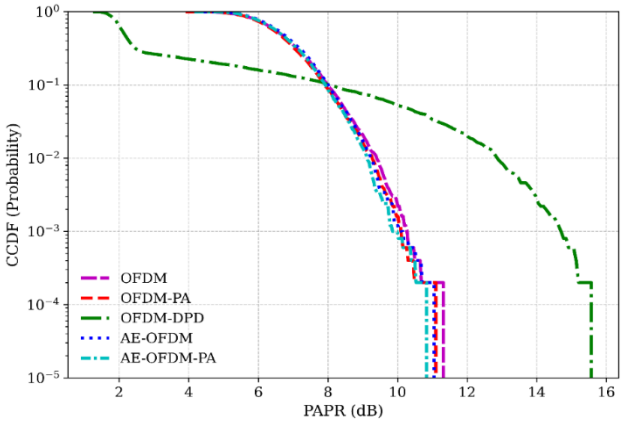

Figure 12. CCDF of PAPR for different OFDM-based systems

3.5. Computational complexity analysis

Table 2 presents the complexity analysis of the AE-OFDM-PA system. The evaluation considers the number of trainable parameters (memory cost) and the floating-point operations (FLOPs, representing execution cost) associated with the neural network layers, which define the model's main computational load. The total complexity of the AE is obtained by summing its encoder and decoder components, resulting in approximately 66.88 thousand FLOPs per OFDM symbol during inference and 57,938 trainable parameters.

Table 2 Computational complexity of the proposed AE-OFDM-PA network

Layer	Input size N_{in}	Output size N_{out}	Multiplications (flops)	Trainable parameters
		AE-Tx		
Dense 1	16	160	2560	2720
Dense 2	160	160	25600	25760
Dense 3	160	2	320	322
		AE-Rx		
Dense 4	64	160	10240	800
Dense 5	160	160	25600	25760
Dense 6	160	16	2560	2576
	Total per OFDM symbol		66.88 K flops	57938

Non-neural operations, such as the IFFT, PA, and FFT, are excluded from this analysis since they contain no trainable parameters and are common to all OFDM-based systems. Compared with the conventional DPD approach, the AE-OFDM-PA exhibits a higher computational cost but achieves significantly improved performance across all key metrics, including BLER, ACLR, and PAPR.

Although the DPD is computationally lightweight, relying on only a few polynomial coefficients, the AE uses its additional complexity strategically to perform end-to-end joint optimization. This allows it to handle both modulation design and PA linearization simultaneously. Despite being built with a modest architecture based on dense layers, the proposed model remains among the least complex deep learning solutions at the physical layer, avoiding the heavy computational load typically associated with recurrent neural network (RNN) or transformer-based designs [28]. This balanced trade-off between complexity and performance justifies the AE's adoption, offering superior spectral efficiency, robustness, and nonlinearity mitigation while maintaining practical computational feasibility.

4. CONCLUSION

This work introduces a novel end-to-end autoencoder framework for linearizing power amplifiers in OFDM systems, jointly addressing PA nonlinearity and channel impairments under unknown CSI conditions. Unlike conventional DPD schemes, the proposed AE-OFDM-PA learns to linearize the PA response directly from data without relying on prior modeling assumptions, making it inherently robust to both PA nonlinearities and channel distortions.

Our AE-OFDM-PA system demonstrates a significant performance improvement over conventional approaches, achieving a BLER improvement of over 70× compared to the uncompensated OFDM-PA system at an IBO of 3 dB, an ACLR gain of approximately 11.5 dB over conventional memory polynomial DPD, and a moderate reduction of PAPR. These results underscore the autoencoder's capability to automatically learn optimal symbol representations and compensate for complex distortions without relying on traditional model-based predistortion techniques.

While the study is based on synthetic data and a simplified single-path Rayleigh fading channel, the incorporation of channel impairments allows evaluation of PA predistortion under more realistic conditions. Future work may extend this framework to PAs with memory effects, MIMO systems, wideband fading channels, or hardware-in-the-loop implementations, further validating its applicability in practical deployments. Overall, this study demonstrates the strength, flexibility, and novelty of the proposed end-to-end learning method, providing a compelling alternative to classical PA compensation strategies and paving the way for intelligent, data-driven communication system design under unknown CSI.

ACKNOWLEDGMENTS

The authors would like to thank the research team and the LTT Laboratory, Faculty of Technology, University of Tlemcen, for their valuable support during this work.

FUNDING INFORMATION

Authors state no funding involved.

AUTHOR CONTRIBUTIONS STATEMENT

This journal uses the Contributor Roles Taxonomy (CRediT) to recognize individual author contributions, reduce authorship disputes, and facilitate collaboration.

Name of Author	C	M	So	Va	Fo	I	R	D	O	E	Vi	Su	P	Fu
Meryem Mamia Benosman	✓	✓	✓	✓	✓	✓		✓	✓	✓	✓			✓
Mohammed Yassine Bendimerad	✓	✓		✓	✓	✓		✓	✓	✓		✓	✓	
Fethi Tarik Bendimerad	✓	✓		✓	✓	✓				✓	✓	✓	✓	

C : **C**onceptualization
M : **M**ethodology
So : **So**ftware
Va : **Va**lidation
Fo : **Fo**rmal analysis
I : **I**nvestigation
R : **R**esources
D : **D**ata Curation
O : Writing - **O**riginal Draft
E : Writing - Review & **E**diting
Vi : **Vi**sualization
Su : **Su**pervision
P : **P**roject administration
Fu : **Fu**nding acquisition

CONFLICT OF INTEREST STATEMENT

Authors state no conflict of interest.

INFORMED CONSENT

This study does not involve any identifiable personal data or human participants. Therefore, informed consent was not required.

ETHICAL APPROVAL

This study did not involve any experiments on human or animal subjects, and therefore ethical approval was not required.

DATA AVAILABILITY

Data availability is not applicable to this paper as no new data were created or analyzed in this study.

REFERENCES

[1] "Cisco Annual Internet Report (2018-2023)" 2020. [Online]. Available: https://ieeemilestones.ethw.org/File:Ref10-Cisco_Annual_Internet_Report_White-Paper_March-2020.pdf (accessed: Dec. 15, 2024).

[2] ITU-R Report M.2410-0, "Minimum requirements related to technical performance for IMT-2020 radio interface(s)," *International Telecommunication Union*, Geneva, Switzerland, Nov. 2017. [Online]. Available: https://www.itu.int/dms_pub/itu-r/opb/rep/R-REP-M.2410-2017-PDF-E.pdf

[3] E. Dahlman, S. Parkvall, and J. Sköld, *5G NR: The Next Generation Wireless Access Technology*. Amsterdam, The Netherlands: Elsevier, 2020.

[4] N. M. A. E. D. Wirastuti, N. P. L. Anggitiadewi, and N. Pramaita, "Pulse shaping methods for inter carrier interference reduction in OFDM system," *TELKOMNIKA (Telecommunication Computing Electronics and Control)*, vol. 18, no. 5, pp. 2276–2287, Oct. 2020, doi: 10.12928/telkomnika.v18i5.13840.

[5] X. Tang, Z. Tan, L. Xiao, M. Zhao, and Y. Li, "A new approach to dealing with the PAPR problem for OFDM systems via deep learning," in *2022 14th International Conference on Wireless Communications and Signal Processing (WCSP), IEEE*, Nov. 2022, pp. 252–256, doi: 10.1109/WCSP55476.2022.10039468.

[6] M. Liu *et al*., "Neural network-assisted DPD of wideband PA nonlinearity for sub-nyquist sampling systems," *Sensors*, vol. 25, no. 4, p. 1106, Feb. 2025, doi: 10.3390/s25041106.

[7] D. J. G. Mestdagh, J. L. Gulfo Monsalve, and J. -M. Brossier, "GreenOFDM: a new selected mapping method for OFDM PAPR reduction," *Electronics Letters*, vol. 54, no. 7, pp. 449–450, Apr. 2018, doi: 10.1049/el.2017.4743.

[8] Y. A. Jawhar *et al*., "A review of partial transmit sequence for PAPR reduction in the OFDM systems," *IEEE Access*, vol. 7, pp. 18021–18041, 2019, doi: 10.1109/ACCESS.2019.2894527.

[9] M. Rakshit, S. Bhattacharjee, G. Garai, and A. Chakrabarti, "A novel differential evolution algorithm for tone reservation based peak to average power ratio reduction technique in orthogonal frequency division multiplexing systems," *Swarm and Evolutionary Computation*, vol. 72, p. 101086, Jul. 2022, doi: 10.1016/j.swevo.2022.101086.

[10] M. González-Rodríguez, C. Collado, J. M. González-Arbesú, J. Mateu, G. Montoro, and P. L. Gilabert, "Tone injection-based cancellation technique for nonlinear distortion reduction of modulated signals in BAW resonators," *Microwave and Optical Technology Letters*, vol. 63, no. 3, pp. 781–786, Mar. 2021, doi: 10.1002/mop.32670.

[11] J. H. Jon and C. W. Han, "Reduction of signal envelope fluctuations in OFDM systems using ACE with double extension," *Wireless Personal Communications*, vol. 132, no. 2, pp. 1177–1192, 2023, doi: 10.1007/s11277-023-10652-5.

[12] H. Duan, M. Versluis, Q. Chen, L. C. N. de Vreede, and C. Gao, "TCN-DPD: parameter-efficient temporal convolutional networks for wideband digital predistortion," in *2025 IEEE/MTT-S International Microwave Symposium - IMS 2025, IEEE*, Jun. 2025, pp. 1103–1106, doi: 10.1109/IMS40360.2025.11103923.

[13] W. S. Costa, J. L. A. Samatelo, H. R. O. Rocha, M. E. V. Segatto, and J. A. L. Silva, "CNN direct equalization in OFDM-VLC systems: evaluations in a numerical model based on experimental characterizations," *Photonic Network Communications*, vol. 45, no. 1, pp. 1–11, 2023, doi: 10.1007/s11107-022-00987-7.

[14] S. Wang, M. Geng, C. Yu, and J. Cai, "Improved behavioral modeling using augmented LSTM networks for ultra-broadband mmWave PA," *Microwave and Optical Technology Letters*, vol. 65, no. 4, pp. 961–968, Apr. 2023, doi: 10.1002/mop.33297.

[15] N. E. West and T. O'Shea, "Deep architectures for modulation recognition," in *2017 IEEE International Symposium on Dynamic Spectrum Access Networks (DySPAN), IEEE*, Mar. 2017, pp. 1–6, doi: 10.1109/DySPAN.2017.7920754.

[16] T. O'Shea and J. Hoydis, "An introduction to deep learning for the physical layer," *IEEE Transactions on Cognitive Communications and Networking*, vol. 3, no. 4, pp. 563–575, Dec. 2017, doi: 10.1109/TCCN.2017.2758370.

[17] D. Baran, "Energy-efficient design techniques for LUT based adaptive digital pre-distorters," *Microelectronics Journal*, vol. 141, p. 105976, Nov. 2023, doi: 10.1016/j.mejo.2023.105976.

[18] J. Ren, Z. Xu, and X. Wang, "A hybrid memory polynomial digital predistortion model for RF transmitters," *Integration*, vol. 100, p. 102285, Jan. 2025, doi: 10.1016/j.vlsi.2024.102285.

[19] Y. Wu *et al*., "MP-DPD: low-complexity mixed-precision neural networks for energy-efficient digital predistortion of wideband power amplifiers," *IEEE Microwave and Wireless Technology Letters*, vol. 34, no. 6, pp. 817–820, Jun. 2024, doi: 10.1109/LMWT.2024.3386330.

[20] H. Al Ibraheemi and M. M. A. Al Ibraheemi, "Wireless communication system with frequency selective channel OFDM modulation technique," *TELKOMNIKA (Telecommunication Computing Electronics and Control)*, vol. 18, no. 3, pp. 1203–1208, 2020, doi: 10.12928/TELKOMNIKA.v18i3.14683.

[21] B. Taha, H. A. Fayed, M. H. Aly, and M. Mahmoud, "A reduced PAPR hybrid OFDM visible light communication system," *Optical and Quantum Electronics*, vol. 54, no. 12, p. 815, Dec. 2022, doi: 10.1007/s11082-022-04219-0.

[22] H. Sohtsinda, "Joint channel and transmit amplifier approach for dynamic power allocation in MIMO-OFDM systems (in French: Approche conjointe canal et amplificateur d'émission pour l'allocation dynamique de puissance dans les systèmes MIMO-OFDM)," Universite de Poitiers, 2017.

[23] X. Lu *et al*., "A low-computational-complexity digital predistortion model for wideband power amplifier," *Sensors*, vol. 24, no. 21, p. 6941, Oct. 2024, doi: 10.3390/s24216941.

[24] A. Rathnayake, L. Silva, H. Rezaei, and N. Rajatheva, "Augmented-LSTM and 1D-CNN-LSTM Models for Linearization of Wideband Power Amplifiers," *2023 IEEE 34th Annual International Symposium on Personal, Indoor and Mobile Radio Communications (PIMRC). IEEE*, pp. 1–6, Sept. 05, 2023, doi: 10.1109/pimrc56721.2023.10294019.

[25] L. Xin, J. Chen, W. Zhao, J. Hua, G. Xu, and T. Liu, "Bidirectional temporal convolutional neural network model for digital

predistortion of RF power amplifier," *2025 International Conference on Microwave and Millimeter Wave Technology (ICMMT). IEEE*, pp. 1–3, May 19, 2025. doi: 10.1109/icmmt65948.2025.11187522.
[26] K. Davaslioglu, T. Erpek, and Y. E. Sagduyu, "End-to-end autoencoder communications with optimized interference suppression," *arXiv*, 2021, doi: 10.48550/arXiv.2201.01388.
[27] T. Erpek, T. J. O'Shea, Y. E. Sagduyu, Y. Shi, and T. C. Clancy, "Deep learning for wireless communications," *arXiv preprint*, 2020, doi: 10.48550/arXiv.2005.06068.
[28] C. Zhang, P. Patras and H. Haddadi, "Deep learning in mobile and wireless networking: a survey, " in *IEEE Communications Surveys & Tutorials*, vol. 21, no. 3, pp. 2224-2287, thirdquarter 2019, doi: 10.1109/COMST.2019.2904897.

BIOGRAPHIES OF AUTHORS

Meryem Mamia Benosman received the M.Sc. degree in Networks and Telecommunications from the Faculty of Technology, University of Tlemcen, Algeria, in 2018. In the same year, she was admitted to the National Doctoral Program in Communication and Wireless Networks at the University of Tlemcen. She is currently pursuing her Ph.D. at the Telecommunications Research Laboratory (LTT), Faculty of Technology, University of Tlemcen, Algeria. Her research interests include wireless communication systems, OFDM-based technologies, power amplifier linearization, PAPR reduction techniques, and the application of artificial intelligence in communication systems. She can be contacted at email: meryemmamia.benosman@univ-tlemcen.dz.

Mohammed Yassine Bendimerad received his B.Sc. degree in Electrical and Electronic Engineering, as well as his M.Sc. and Ph.D. degrees in Telecommunication and Wireless Communication Technologies from the University of Tlemcen, Algeria, in 2010, 2012, and 2016, respectively. In 2016, he joined the University of Bechar as an Assistant Professor in the Department of Electrical and Electronic Engineering. He is currently a Professor (since June 2025) in the Telecommunications Department and a research member of the Digital Communication Team at the LTT Laboratory of Telecommunications at the University of Tlemcen. His research interests include wireless communication and mobile networks, energy efficiency in wireless systems, and artificial intelligence for optimizing communication protocols. He has authored several papers published in international conferences and journals, including those indexed by IEEE. Additionally, he has participated in various national and international research projects, such as the PRFU, PHC-TASSILI, and ACADEMY Projects, and collaborates as a reviewer for international journals included in the JCR. He can be contacted at email: yassine.bendimerad@univ-tlemcen.dz.

Fethi Tarik Bendimerad received the Engineering degree in Electronics from the University of Science and Technology of Oran (USTO), Algeria, in 1983, the Diplôme d'Études Approfondies (DEA) in Telecommunications from the University of Nice–Sophia Antipolis, France, in 1984, and the Ph.D. degree in Telecommunications from the same university in 1989. His Ph.D. was officially recognized as equivalent to the Doctorat d'État in June 1992. He is currently a Professor with the Faculty of Engineering, University of Tlemcen, Algeria. He is also the Director of the Telecommunications Research Laboratory at the University of Tlemcen, and previously served as the Director of the Institute of Electronics at the same university. His research interests include wireless communications, signal processing, and advanced telecommunication systems. He has supervised several Ph.D. students and contributed to numerous national and international research projects. He is the author of several publications in reputable journals and conferences and regularly serves as a reviewer for scientific journals. He can be contacted at email: fethitarek.bendimerad@univ-tlemcen.dz.